SCIENTIFIC PAPER

EXPERIMENTAL STUDY OF SOLAR AIR HEATER WITH C SHAPED RIBS COATED WITH ZEOLITE

Sureshkumar Petchimuthu[1*], Sathiya Moorthy Rajendran[2]

[1*] Department of Mechanical Engineering, Government College of Engineering, Tirunelveli 627007, India

[2]Department of Mechanical Engineering,
Anna University Regional Campus, Coimbatore 641046, India

https://doi.org/10.2298/CICEQ231230010P

Received 30.12.2023.

Revised 11.3.2024.

Accepted 27.3.2024.

[*] Corresponding author: email:ppskumar200@gmail.com, mobile number: +916369009050

Abstract

A study was conducted to determine the heat transmission rate and friction properties of a solar air heater's (SAH) absorber by including c-shaped rib, with and without perforations, and the efficiency of this absorber with and without zeolite coating was investigated. This research is carried out by varying Reynolds numbers (Re) ranges between 3000 to 18000, height of the C-shaped rib (e) ranges between 2 mm to 4 mm, and the embedded hole diameter in the c-shaped rib ranges between 1 mm to 3 mm. The impact of rib height, hole diameter, and zeolite coating on thermal efficiency and Nusselt number is compared to a flat channel under the same flow environments. A strong secondary flow is created by the free shear layer reattaching more often at higher rib heights, and a smaller hole can exaggerate heat transfer and enhance the cross-flow effect. The thermal efficiency and Nusselt number of the solar air heater with c-ribs (Rib height = 4mm and hole diameter = 1mm) and zeolite coating on the absorber increased by 29.67% and 62.16% over the flat absorber. Ribs 4mm high can increase duct friction by up to 3.1 times compared to a smooth duct.

Keywords: C-shaped ribs, Perforations, Zeolite coating, Thermal performance, Friction factor.

Highlights

- Improve the performance of a SAH using C-ribs with zeolite coating on the absorber plate.
- A high rib height promotes increased turbulence and mixing of air flowing through the SAH duct.
- Smaller hole can exaggerate heat transfer and enhance the cross-flow effect.
- Zeolite coatings, serve to enhance the thermal performance by desorption and adsorption processes.

INTRODUCTION

Solar air heaters are a fundamental part of solar energy utilisation systems. They are designed to absorb incoming solar light and convert it into thermal energy at the absorber plate. The heated absorber plate transfers thermal energy to the air passing through the duct via convection. The thermal energy stored in the hot absorber plate is transferred to the air because of the temperature disparity. This process heats up the air as it passes through the SAH. These SAH systems are used in various applications for heating purposes, including space heating, preheating air for combustion processes, drying crops, desalination (evaporating seawater to produce fresh water), and water heating. The efficiency of flat SAHs is low because there is not enough convective heat transfer among the fluid and the absorber. Consequently, the temperature of the absorber rises, and more heat emission to the atmosphere is higher. The existence of viscous sub-layer is most often due to poor heat transfer; this layer can be eliminated by roughening the absorber. Various techniques, including the incorporation of fins, artificial roughness, and packed beds within ducts, have been proposed as methods to enhance thermal performance. Implementing roughened surfaces on the absorber plate, such as ribbed or corrugated surfaces, disrupts laminar airflow and promotes turbulence. This improves the transfer of heat from the absorber to the air. Applying selective coatings to the absorber plate maximizes solar absorption while minimizing thermal radiation losses, improving overall efficiency.

Yadav et al. [1] tested the impact of a circular rib positioned in an angular arc approached and discovered that heat transmission and friction are greater than the flat one. Lanjewar et al. [2] investigation done on the influence of W - shaped ribs as an artificial elements. The author found that thermo-hydraulic performance was extreme at a slant of attack is 60^0. Pandey et al. [3] explored the impact of “relative roughness height, arc angle, pitch, width, gap distance on “Nusselt number (Nu), and friction factor (f)” using multiple-arc shaped ribs fixed over absorber. The author found that Nu = 5.85 and f = 4.96 is superior to flat channel. Saini et al. [4] probed the impact of ribs with dimple forms over Nusselt number and friction factor. Unlike flat absorbers, ribs considerably improved Nu and friction qualities. Varun et al. [5] researched impact of "inclined and transverse ribs" above the absorber were tested. At “relative roughness pitch =8”, it was found that a higher thermal efficiency was reached. Kumar et al. [6] experimented with the impact of separate “W-shaped” ribs and discovered that “Nusselt number” was 1.67, and “friction” was 1.82 attained at an angle of attack is 60^0. Sahu and Prasad [7] theoretically investigated arc-shaped wire

protrusions over the absorber. The author reported that the roughness height is 0.0422 the greatest improvement in exergetic efficiency 56% greater as compared to flat absorber.

Jin et al. [8] has numerically analyze the impact of an artificial roughness many "V-shaped ribs" over the absorber. The author stated that "V-shaped ribs" create "stream wise helical vortex flows" that augment the performance of SAHs. Yadav and Bhagoria [9] executed a numerical study on the square-separated transverse rib and revealed that square-separated transverse rib along relative roughness, pitch, and height gives better thermo-hydraulic performance.

Aharwal et al. [10] researched the impact of "gap width, and position" on "heat transfer, and friction factor" having a slanted continuous rib. The optimal "width" is 1.0 and the "position" of 0.25 obtained better thermo hydraulic performance. Sahu and Bhagoria [11] explored the effect of heat transmission coefficient in 90^0 broken ribs and it was found that the thermal efficiency ranges from 51 to 83.5%. Hans et al. [12] studied the outcome of several "v-ribs" on the absorber of a SAH. The study included Re from 2000 to 20000, e/D from 0.019 to 0.043, P/e from 6 to12, a from 30 to75° and W/w from1to10. The author found that heat transfer was 6 and friction was 5 times as greater compared with the flat absorber. Ghritlahre et al. [13] the study examined the thermal performance and heat transfer of an arc-shaped roughened SAH with two different airflow orientations: apex up and apex down. The experiments were conducted using different mass flow rates, spanning from 0.007 to 0.022 kg/s. The roughness parameters taken into study included "relative roughness pitch, relative roughness height, rib roughness, and arc angle". The heat transfer in the apex up configuration was 33.2% more efficient compared to the apex down arrangement. These results suggest that the apex up airflow with wire rib roughness absorber is more efficient than the apex down airflow SAH.

Agrawal et al. [14] empirically studied the impact of double arc reverse formed along consistent gap and discovered "Nusselt Number" of 2.85, and the "friction factor", 2.42 higher than a plane absorber. Singh et al. [15] examined the effect of several "arc" ribs over thermal performance. The author discovered that the huge increment of "Nusselt number", 5.07, and "friction factor", 3.71, was higher than the flat one.

Kumar et al. [16] experimentally researched the impact of nano material interfering with black paint covering on an absorber. It is concluded that the entropy formation rises with rises in the rate of flow. Exergy effectiveness for BP-2 is discovered to be 4.27% greater than

BP-1. Jelonek et al. [17] studied the effectiveness of new sand plastered and sand packed (SCSF) polycarbonate sheet SAC. It was discovered that the SAC with storing offered 39% and 20% greater efficiency than other two. After an extensive survey, it could be inferred that researchers have worked on varying the geometric parameters like Rib roughness, height, pitch and coating over the absorber for better thermal performance in SAHs.

In light of the foregoing, the present study was conducted with the objective of determining Nusselt number and friction characteristics over the heated surface using a c-shaped rib with and without holes embedded on it to generate vortex as a roughness element on the absorber surface. The C-shaped rib configuration can induce strong vortices and turbulence in the boundary layer flow. This enhanced turbulence promotes better mixing and heat transfer amid the fluid and the solid surface, leading to improved convective heat transfer coefficients. Compared to other rib configurations, such as rectangular or trapezoidal ribs, the C-shaped rib may offer the advantage of lower pressure drop. The streamlined shape of the C rib could help minimize flow resistance while still effectively enhancing heat transfer. The experiment was also carried out by adding a zeolite coating to the absorber plate. Researchers have looked at a wide variety of roughness element forms and sizes, but none have made an effort to test the effects of the current geometry and coating on heat convection.

EXPERIMENTAL INFORMATION

Experimental System

The effects of several "c-shaped" ribs on heat transfer and frictional properties of SAH have been studied in the experiment. Figure 1 provides a graphical depiction of the experiment. The air duct is split into three distinct areas: entrance, testing, and exit. Measurements for the entire duct are 1750 mm, and testing section length is 1000 mm having corresponding 80 mm hydraulic diameter. The lengths of the entering and exiting segments are 500 mm and 250 mm, respectively. To determine proper entry and exit dimensions, ASHRAE 93-77 is used as a reference. This shows that the minimum inlet and outlet lengths for the zig zag flow regime should be $5\sqrt{WH}$ and $2.5\sqrt{WH}$, respectively. Improved airflow across absorber's surface has been achieved by inserting guide vanes at the inlet. Wood was chosen as the duct's primary construction material because it is affordable, abundant, and good at insulating. GI sheet absorber plate of 3 mm thickness is made. The upper surface of

the absorber is artificially roughened using riveted c-shaped ribs. The absorber plate is made as the duct bottom wall, and the glass wool is used to insulate the sidewalls.

In order to measure the input and output air temperatures, thermocouples have been installed. Calibrated K-type thermocouples with digital displays, showing output in degrees Celsius with an accuracy of 0.1^0C was employed to determine air temperature and absorber plate temperatures across multiple locations. A standard thermometer was used to calibrate the thermocouples. The position of the twelve thermocouples installed at regular intervals to gauge the average temperature of the absorber is shown in Figure 2 (a). A calibrated orifice metre coupled with U-tube manometer is included for determining the airflow rate. A Pitot tube was utilised for orifice plate calibration. The inlet flow rate has been regulated by including flow regulating valve in the entry. The pressure downfall in the test area is measured with a digital micromanometer. Rib placements above the absorber are shown in Figure 2 (b).

Figure 1

Figure 2

Experimental procedure

Prior to the commencement of the experiment, component parts and instruments were tested for functionality. Under steady-state conditions, the requisite heat transfer research investigations were carried out. The airflow rate ranged between 0.0064 kg/s and 0.0386 kg/s with four in-between values to represent all possible variations of the Reynolds number from 3000 to 18000 respectively.

The average solar intensity (I) is measured as 800 W/m^2 at Bodinayakanur, Tamil Nadu, India during the month of May2023. Since the working fluid is air, Density, Specific heat, Thermal conductivity and Dynamic viscosity are 1.225 Kg/m^3, 1006 J/kg K, 0.0262 W/m K, 1.81×10^{-5} Kg/m s, respectively.

The following variables are assessed during experimentation:

(1) Air Temperature at entry.
(2) Air Temperature at exit.
(3) Mean temperature of the absorber plate.
(4) Pressure drop across test section.

Figure 3

Data Reduction

The rate of flow of air, the transfer of heat to the air, Nusselt number, Heat transfer coefficient and friction factor are quantified with available data from present study.

The necessary parameters are evaluated as per the highlighted References Deceased John Duffie and Beckman William [18] using formulae.

3.1 Mass flow rate can be measured as

$$m = \rho A V \tag{1}$$

Where, $A = \frac{\pi}{4} d^2$

3.2 Heat transfer can be calculated with the relation

$$Q = m\, c_p\, (T_0 - T_i) \tag{2}$$

3.3 Thermal efficiency is determined from (3)

$$\eta = \frac{Q}{I\, A_c} \tag{3}$$

Where, A_c = Length of the absorber × Width of the absorber

3.4 Heat transfer coefficient can be ascertained by (4)

$$h = \frac{Q}{A_c\,(T_p - T_f)} \tag{4}$$

Where

$$T_f = \frac{(T_i + T_o)}{2}$$

$$T_p = \frac{(T_1 + T_2 + T_3 + T_4 + T_5 + T_6 + T_7 + T_8 + T_9 + T_{10} + T_{11} + T_{12})}{12}$$

3.5 Nusselt number measurement for roughened absorber

$$Nu = \frac{h\, D_h}{k} \tag{5}$$

3.6 Friction factor measurement for roughened absorber

$$f = \frac{D_h \Delta P}{2 L V^2 \rho} \quad (6)$$

Validity test

The experimentally obtained Nusselt number and Friction factor values in flat are compared with value computed through "Dittus–Boelter" Equation and "Modified Blasius" Equation, respectively.

Dittus-Boelter formula

$$Nu_s = 0.023\, Re^{0.8} Pr^{0.4} \quad (7)$$

Modified Blasius formula

$$f_s = 0.085\, Re^{-0.25} \quad (8)$$

Figure 4

Figures 4 (a) and (b) graphically represent the experimental and mathematically established Nu and f, respectively. The mean deviation of Nu is 2.65%, and the mean deviation of friction factor values is 2.57%. This confirms a high degrees of conformity between predicted and experimental results, thus validating the setup of the experiment.

Uncertainty Analysis

Uncertainty analysis is a useful and efficient tool for developing and planning experiments. Following equations are then utilized to determine the uncertainty measurement.

$$\mathrm{W_R} = \sqrt{\left[\left(\frac{\partial \mathrm{R}}{\partial \mathrm{x_1}} \mathrm{w_1}\right)^2 + \left(\frac{\partial \mathrm{R}}{\partial \mathrm{x_2}} \mathrm{w_2}\right)^2 + \ldots\ldots\ldots + \left(\frac{\partial \mathrm{R}}{\partial \mathrm{x_n}} \mathrm{w_n}\right)^2\right]} \quad (9)$$

Where,

X1, X2 … Xn= the independent variables,

W1, W2 … Wn= the uncertainties in the independent variables

Thermal efficiency, Nu and friction factor are uncertainty is 3.20, 3.32 and 3.26%, respectively, which is within acceptable ranges. The following uncertainties are associated with the measurements: Mass flow rate: ± 0.001 m³/hr, Temperature: ± 0.1°C, Radiation: ± 1 W/m², Pressure Drop: ± 0.098 Pa, Duct height: ± 0.1 mm, and Absorber plate length: ± 0.6 mm.

RESULTS AND DISCUSSION

The significance of rib height, hole diameter, and zeolite coating at heat transmission and friction qualities of a roughened absorber have been investigated.

Heat Transfer Properties

The "Heat Transfer Properties" section of the study focuses on examining the thermal characteristics and performance of the SAH system under investigation. This part aims to gives a detailed analysis of the heat transfer processes occurring within the SAH, and their impact on overall system efficiency.

Effect of Reynolds Number (Re)

As the Reynolds number goes up, we consistently see a rise in the Nusselt number. This happens because the viscous layer near the surface gets thinner with higher Reynolds numbers. This thinner layer allows for more heat transfer. On the other hand, the friction factor consistently falls with increasing Reynolds number. In smooth ducts with fully developed flow, this decrease is due to less resistance from the thinned viscous sublayer. However, it also means a larger pressure drop along the duct, requiring more pumping power. Adding roughness to the absorber plate disrupts the smooth flow, creating more turbulence. This turbulence increase manifests as a higher friction factor compared to a smooth plate.

Effect Of Rib Height (e)

The effect of rib height (e) on thermal efficiency (η) and Nusselt number (Nu) for Re between 3000 and 18000 is depicted in Figure 5 (a) and (b). The thermal efficiency of the SAH is directly proportional to the flow rate at the entry. As mass flow rates rise, thermal efficiency increases because more heat is removed by the working fluid. As the rib height (e) is increased, Nusselt number and thermal efficiency increase due to a secondary flow created by the free shear layer at a higher rib height. A high rib height promotes increased turbulence and mixing of air passing through the SAH duct. Turbulence enhances heat transfer by disrupting laminar flow and promoting convective heat exchange between the hot absorber plate and the air. Taller ribs provide a larger surface area for heat transfer between the absorber and the airflow. This increased surface area allows for greater contact between the heated absorber and the air, facilitating more efficient heat transfer. In contrast, a low rib height may result in less turbulence and mixing, leading to reduced heat transfer enhancement

compared to higher rib heights. Shorter ribs offer less surface area for heat transfer, potentially limiting the effectiveness of convective heat exchange within the SAH duct. Lower rib heights typically result in lower pressure drop and energy losses compared to higher rib heights. However, the lower rib height reduced heat transfer efficiency. In addition, by including a c-shaped rib, local wall turbulence has been induced in the heat transmission region. The thermal resistance falls significantly as the heat transfer improves. The main flow impinges on the surface as rib height increases, increasing rate of heat transfer for all values of Re. Reduction in heat transfer from surface of the absorber is observed if the rib height is beyond 4 mm because the free shear layer cannot rejoin. Reduced rib height allows reconnected air to travel further before colliding with subsequent ribs, enabling the regrowth of a viscous sub-layer on a localised region of the heater's surface. The regrowth of the boundary layer causes a decrease in the Nu, causing adverse effect on heat transfer from the absorber.

Figure 5

Effect Of Hole Diameter (D)

In Figures 5 (c) and (d), we examine the way the thermal efficiency and the Nusselt number change as a consequence of hole diameter (D) for Re range of study. As the hole diameter increases, it is evident that thermal efficiency decreases. A smaller opening can increase the cross-flow effect and heat transfer rates. The c-shaped configuration with a 1 mm hole diameter has the highest exit temperature because the air has to go through a smaller hole before it moves out, so it stays in the test part for a longer duration. Additionally, it generates several small vortices in the rib region, which in turn increase the turbulence. Increased turbulence is responsible for the better thermal efficiency and higher Nusselt number. In addition smaller hole diameters provide a larger surface area for heat transfer between the absorber and the airflow. This increased surface area facilitates more effective convective heat exchange and enhances heat transfer efficiency within the SAH duct. Larger holes do not contribute to enhance heat transmission because of the sluggish flow regime, and Higher hole diameters offer less surface area for heat transfer, potentially limiting convective heat exchange and reducing heat transfer efficiency compared to systems with smaller hole diameters.

Effect Of Zeolite Coating

Figures 6 (a) and (b) illustrate the variation in thermal efficiency and Nusselt number of the zeolite coated absorber for different Re values. The rib height of 4mm and embedded hole diameter of 1mm with zeolite coating have a better heat transfer rate. Desorption and adsorption techniques are used by the zeolite for storing and releasing heat. In the context of heat storage, adsorption refers to the process where molecules of a gas or vapor adhere to the surface of the zeolite. When a zeolite material is exposed to heat, it can adsorb molecules of a specific gas or vapor, typically water vapor or other volatile organic compounds, into its porous structure. This adsorption process is exothermic, meaning it releases heat energy as the molecules are attracted to the surface of the zeolite. Desorption is the reverse process of adsorption. When the zeolite material is subjected to a decrease in temperature or a decrease in pressure, the adsorbed molecules are released from the surface of the zeolite. This desorption process is endothermic, meaning it requires energy input to break the bonds between the molecules and the zeolite surface. The energy required for desorption is typically supplied in the form of heat, which can be provided by solar energy in solar air heater systems. This is because zeolite naturally has an exothermic characteristic, making it an excellent solar collector for use in thermal applications. Zeolite has around 20 to 50% intra-crystalline voids.

A coating of zeolite over the absorber collects the heat from sunlight. Wet air is passed via the air heater to extract and utilise the heat stored in the zeolite coated absorber. This enables the zeolites to dry the air by adsorbing the water from it. The air warms up as a result of the exothermic adsorption. A strong secondary flow is created by the free shear layer reattaching more often at higher rib heights, and a smaller hole can exaggerate heat transfer and enhance the cross-flow effect. Larger holes do not participate in the enhancement of heat transmission due to the stagnant flow regime. The heat transmission is improved as a result of the smaller holes.

Figure 6

Friction Factor Characteristics

Figure (7) shows the impact of hole diameter and rib height over the friction factor in Re range of 3000 to 18000. Blasius correlation is used in computing the friction factor for flat passage. It manifests that the friction factors drop with a raise in Re. This is caused by the thinning of viscous sub layer; Reynolds number increases which is caused by a rise in mean flow velocity when friction factor is lowered.

As Re increases, it results in a decrease in the pressure in the test region. Friction factor varies inversely as the mean square of fluid's velocity and directly related to pressure. Consequently, a rise in mean fluid velocity predominates over a rise in pressure downfall. The friction factor declines in tandem with increasing Re. The friction factor is larger at 4 mm rib height when compared to the one with embedded hole. As the roughness height rises, so does the friction factor. As rib height increases, the flow becomes more turbulent, causing an increase in viscous drag over the absorber and ultimately friction factor rises. Rise in turbulence is not very incisive at lesser rib height values. The holes in the ribs cause an increase in the ratio of open regions. The higher the ratio of the open region, the lower is the pressure within SAH. Since the friction factor is much reduced due to the reduction in pressure loss as compared to ribs without perforations.

Figure 7

Comparison of C- Shaped, V- Shaped and Circular ribs

Compared to V-shaped and circular ribs, C-ribs offer potentially superior heat transfer due to their open face facilitating better air contact with the collector plate. This translates to more efficient heat transfer from the absorber to the air. Additionally, C-shaped ribs might have a lower pressure drop because of the larger flow passage area they create. On the other hand, V-shaped and circular ribs generally have moderate heat transfer and pressure drop characteristics. These have used for space heating in winter session. C-shaped ribs can enhance heat transfer, potentially allowing for a smaller collector size to meet heating needs. This can be beneficial for space-constrained rooftops.

CONCLUSION

These inferences can be made based on the findings of this experimental study.

(1) As Re increases, thermal performance rises and f falls. The Friction and thermal properties of a c-rib are higher when compared to a flat absorber. This is because roughness changes the flow properties, leading to flow separation, the creation of secondary flows, and reattachments.

(2) The thermal efficiency and Nu of the SAH with c-ribs (Rib height = 4mm and hole diameter = 1mm) and zeolite coating on the absorber increased by 29.67% and 62.16% over the flat absorber. A strong secondary flow is created by the free shear layer reattaching more often at higher rib heights, and a smaller hole can exaggerate

heat transfer and enhance the cross-flow effect. Desorption and adsorption techniques are used by the zeolite for storing and releasing heat. This is due to the inherent exothermic property of zeolite which makes it suitable in efficiently harvesting solar energy for heating application.

(3) Ribs 4mm high can increase duct friction by up to 3.1 times compared to a smooth duct. The presence of roughness, the flow becomes more turbulent, causing an increase in viscous drag over the absorber compared to smooth configuration.

Nomenclature

A_c area of collector plate (m^2)

C_p specific heat of air at constant pressure(J/kgK)

D holediameter (mm)

D_h hydraulic diameter (mm)

I incident radiation (W/m^2)

m mass flow rate(kg/s)

p longitudinal pitch

P pressure (Pa)

q heat gain (W)

T_i temperature at entrance (K)

T_o temperature at exit (K)

ΔT difference in temperature (K)

v meanflow velocity (m/s)

Greek Symbols

ρ Specific mass (kg/m^3)

μ Absolute viscosity of working fluid (kg/m-s)

η Thermal efficiency

Subscripts

h hydraulic

i inlet

o outlet

p plate

Abbreviations

f Friction factor

Nu Nusselt number

Pr Prandtlnumber

Re Reynolds number

SAC Solar Air Collector

SAH Solar Air Heater

SCSF Sand Coated and Sand Filled

References

[1] S. Yadav, M.Kaushal, Varun, Siddhartha, Exp. Therm. Fluid Sci. 44 (2013) 34–41. https://doi.org/10.1016/j.expthermflusci.2012.05.011

[2] A. Lanjewar, J.L. Bhagoria, R. Sarviya, Exp. Therm. Fluid Sci. 35 (6) (2011) 986–995. https://doi.org/10.1016/j.expthermflusci.2011.01.019

[3] N. K. Pandey, V.K. Bajpai, Varun, Sol. Energy 134 (2016) 314–326. https://doi.org/10.1016/j.solener.2016.05.007

[4] R.P. Saini, J. Verma, Energy 33 (8) (2008) 1277–1287. https://doi.org/10.1016/j.energy.2008.02.017

[5] Varun, R.P. Saini, S.K. Singal, Renewable Energy 33 (6) (2008) 1398–1405. https://doi.org/10.1016/j.renene.2007.07.013

[6] A. Kumar, J.L. Bhagoria, R.M. Sarviya, Energy Convers. Manage. 50 (8) (2009) 2106–2117. https://doi.org/10.1016/j.enconman.2009.01.025

[7] M.K. Sahu, R.K. Prasad, Renewable Energy 96 (2016) 233–243. https://doi.org/10.1016/j.renene.2016.04.083

[8] D. Jin, M. Zhang, P. Wang, S. Xu, Energy 89 (2015) 178–190. https://doi.org/10.1016/j.energy.2015.07.069

[9] A.S. Yadav, J.L. Bhagoria, Int. J. Therm. Sci. 79 (2014) 111–131. https://doi.org/10.1016/j.ijthermalsci.2014.01.008

[10] K.R. Aharwal, B.K. Gandhi, J.S. Saini, Renewable Energy 33 (4) (2008) 585–596. https://doi.org/10.1016/j.renene.2007.03.023

[11] M.M. Sahu, J.L. Bhagoria, Renewable Energy 30 (13) (2005) 2057–2073. https://doi.org/10.1016/j.renene.2004.10.016

[12] V.S. Hans, R.P. Saini, J.S. Saini, Sol. Energy 84 (6) (2010) 898–911. https://doi.org/10.1016/j.solener.2010.02.004

[13] H.K. Ghritlahre, P.K. Sahu, S. Chand, Sol. Energy 199 (2020) 173–182. https://doi.org/10.1016/j.solener.2020.01.068

[14] Y. Agrawal, J.L. Bhagoria, V.S. Pagey, Mater. Today Proc. 47 (2021) 6067–6073. https://doi.org/10.1016/j.matpr.2021.04.623

[15] A.P. Singh, Varun, Siddhartha, Exp. Therm. Fluid Sci. 54 (2014) 117–126. https://doi.org/10.1016/j.expthermflusci.2014.02.004

[16] R. Kumar, S.K. Verma, M. Singh, Mater. Today Proc. 44 (2021) 961–967. https://doi.org/10.1016/j.matpr.2020.11.006

[17] Z. Jelonek, A. Drobniak, M. Mastalerz, I. Jelonek, Sci. Total Environ. (2020) 141267.

https://doi.org/10.1016/j.energy.2022.125507

[18] B. Bhushan, R. Singh, Sol. Energy 85 (5) (2011) 1109–1118. https://doi.org/10.1016/j.solener.2011.03.007

[19] S. Alfarawi, S.A. Abdel-Moneim, A. Bodalal, Int. J. Therm. Sci. 118 (2017) 123–138. https://doi.org/10.1016/j.ijthermalsci.2017.04.017

[20] A.M. Ebrahim Momin, J.S. Saini, S.C. Solanki, Int. J. Heat Mass Transfer 45 (16) (2002) 3383–3396. https://doi.org/10.1016/S0017-9310(02)00046-7

[21] A. Lanjewar, J.L. Bhagoria, R.M. Sarviya, Energy 36(7) (2011) 4531–4541. https://doi.org/10.1016/j.energy.2011.03.054

[22] S.B. Bopche, M.S. Tandale, Int. J. Heat Mass Transfer 52 (2009) 2834–2848. https://doi.org/10.1016/j.ijheatmasstransfer.2008.09.039

[23] A. standard 93-97, 1977.

[24] R. Kumar, V. Goel, P. Singh, A. Saxena, A.S. Kashyap, A. Rai, J. Energy Storage. 26 (2019) 100978. https://doi.org/10.1016/j.est.2019.100978

[25] F. Afshari, A. Sözen, A. Khanlari, A.D. Tuncer, C. Şirin, Renewable Energy 158 (2020) 297–310. https://doi.org/10.1016/j.renene.2020.05.148

[26] R. Khatri, S. Goswami, M. Anas, S. Sharma, S. Agarwal, S. Aggarwal, Energy Reports 6 (2020) 627–633. https://doi.org/10.1016/j.egyr.2020.11.177

[27] C.D. Ho, H. Chang, R.C. Wang, C.S. Lin, Appl. Energy 100 (2012) 155–163. https://doi.org/10.1016/j.apenergy.2012.03.065

[28] A.A. Farhan, A. Issam M.Ali, H.E. Ahmed, Renewable Energy 169 (2021) 1373–1385. https://doi.org/10.1016/j.renene.2021.01.109

[29] Q.A. Jawad, A.M.J. Mahdy, A.H. Khuder, M.T. Chaichan, Case Stud. Therm. Eng. 19 (2020) 100622. https://doi.org/10.1016/j.csite.2020.100622

[30] R. Azad, S. Bhuvad, A. Lanjewar, Int. J. Therm. Sci. 167 (2021) 107013. https://doi.org/10.1016/j.ijthermalsci.2021.107013

[31] S. Rönsch, B. Auer, M. Kinateder, K. Gleichmann, Chem Eng Technol 43 (12) (2020) 2530-2537. https://doi.org/10.1002/ceat.202000342

Figure captions:

Figure 1.Shows the experiment setup

Figure 2.(a) Thermocouples fixed over the test section and (b) Rib positions over the absorber plate

Figure 3.(a) Pictorial view of e = 4mm, D = 1mm and Zeolite coating, (b) Enlarged view of a Rib Heights and (c) Enlarged view of a Rib Height (e) = 4 mm and Hole Diameters of 1, 2 and 3 mm

Figure 4.(a) Validation of Smooth plate for Nu and(b)Validation of Smooth plate for f

Figure 5. (a)Thermal efficiencyVs Re for rib height, (b)Nusselt number Vs Re for rib height, (c) Thermal efficiency Vs Re for hole diameter and (d) Nusselt number Vs Re for hole diameter

Figure6. (a)Thermal efficiency Vs Re for Zeolite coating and (b) Nusselt number Vs Re for Zeolite coating

Figure 7. Friction factor Vs Re

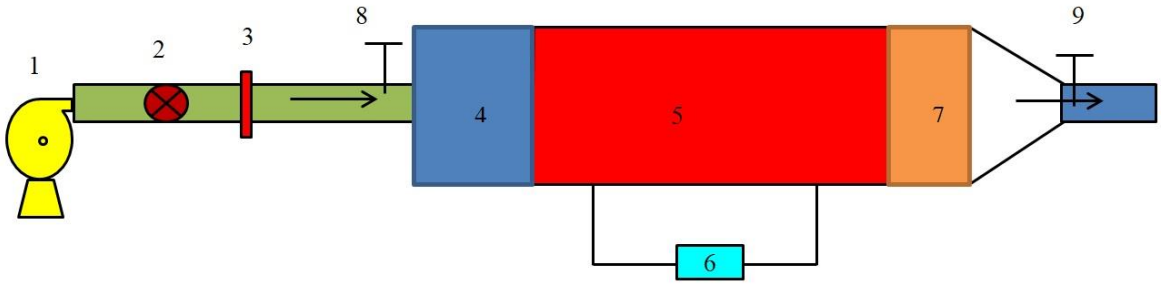

1. Blower
2. Control valve
3. Orifice meter
4. Entrance section
5. Test section
6. Micro manometer
7. Exit section
8. Thermocouple for inlet air temperature
9. Thermocouple for outlet air temperature

Figure 1

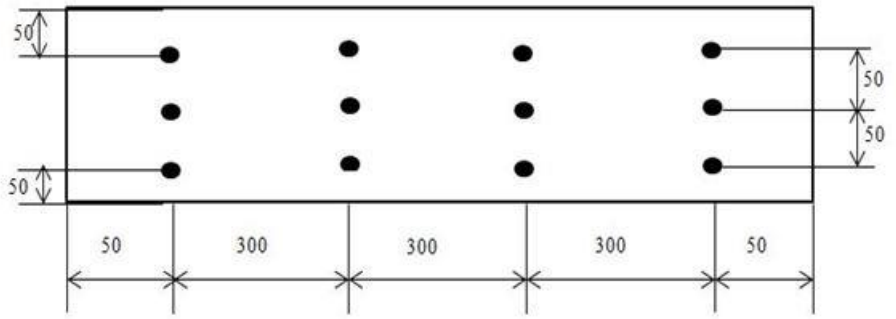

All Dimensions are in mm

(a)

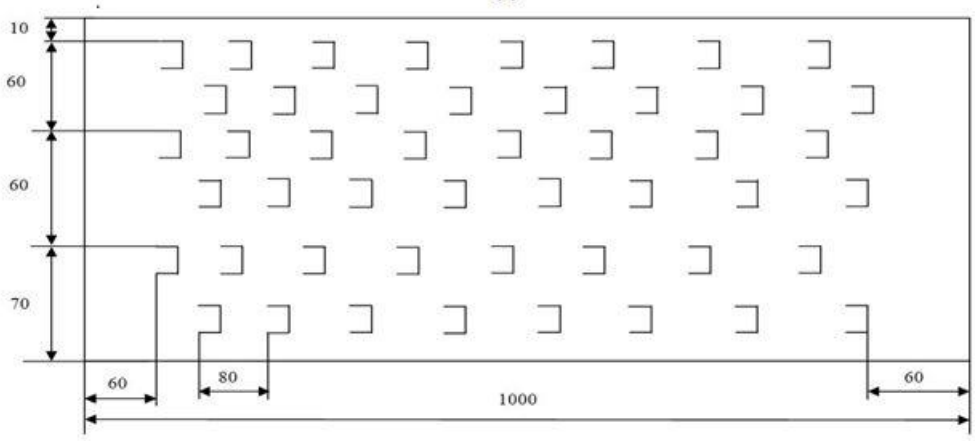

All Dimensions are in mm

(b)

Figure 2

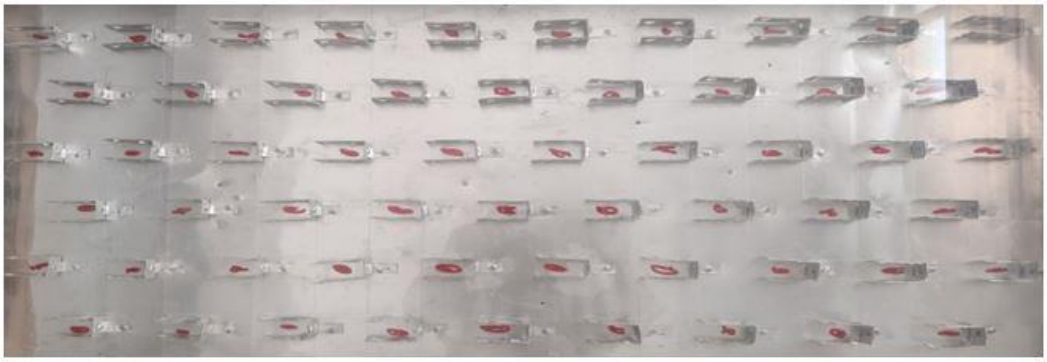

(a)

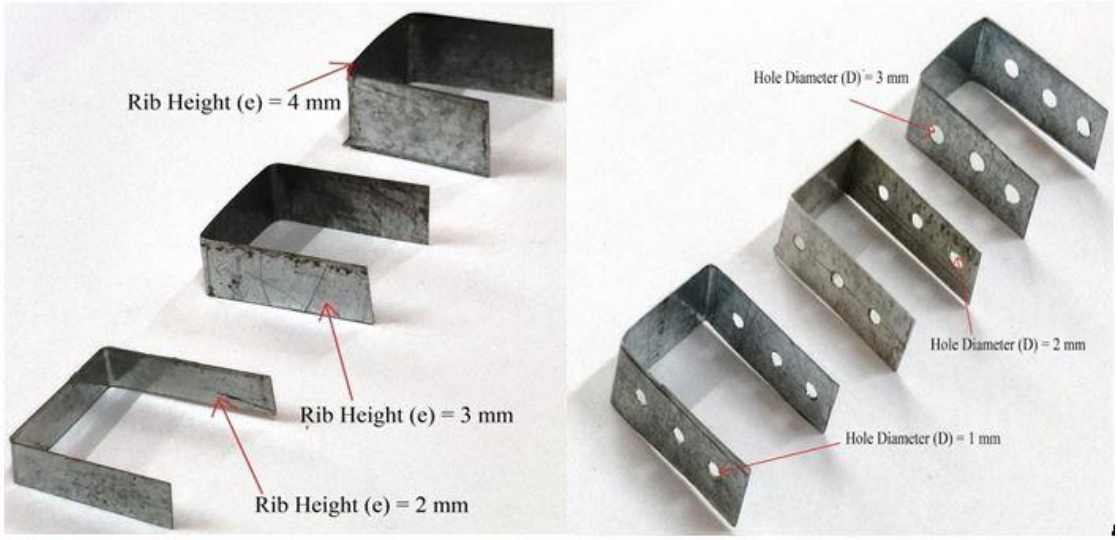
Rib Height (e) = 4 mm
Rib Height (e) = 3 mm
Rib Height (e) = 2 mm
Hole Diameter (D) = 3 mm
Hole Diameter (D) = 2 mm
Hole Diameter (D) = 1 mm

(b) (c)

Figure 3

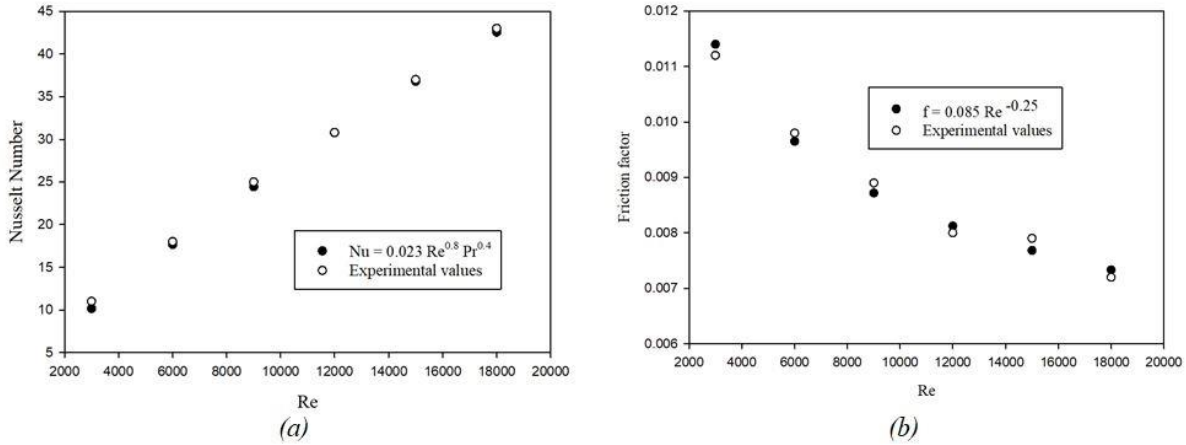
Nusselt Number
Re
Nu = 0.023 Re^0.8 Pr^0.4
Experimental values
(a)
Friction factor
Re
f = 0.085 Re^-0.25
Experimental values
(b)

Figure 4

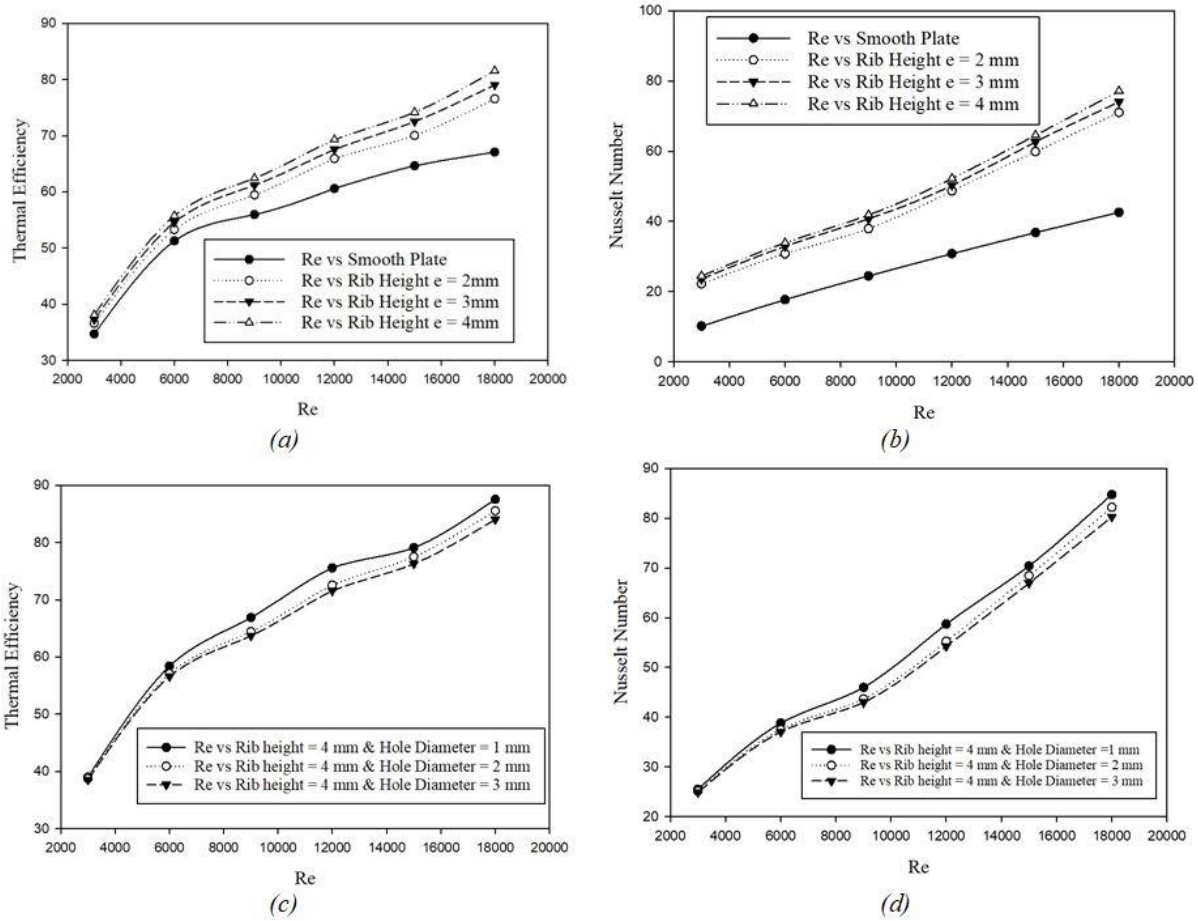
Thermal Efficiency
Re
Re vs Smooth Plate
Re vs Rib Height e = 2mm
Re vs Rib Height e = 3mm
Re vs Rib Height e = 4mm
(a)
Nusselt Number
Re
Re vs Smooth Plate
Re vs Rib Height e = 2 mm
Re vs Rib Height e = 3 mm
Re vs Rib Height e = 4 mm
(b)
Thermal Efficiency
Re
Re vs Rib height = 4 mm & Hole Diameter = 1 mm
Re vs Rib height = 4 mm & Hole Diameter = 2 mm
Re vs Rib height = 4 mm & Hole Diameter = 3 mm
(c)
Nusselt Number
Re
Re vs Rib height = 4 mm & Hole Diameter =1 mm
Re vs Rib height = 4 mm & Hole Diameter = 2 mm
Re vs Rib height = 4 mm & Hole Diameter = 3 mm
(d)

Figure 5

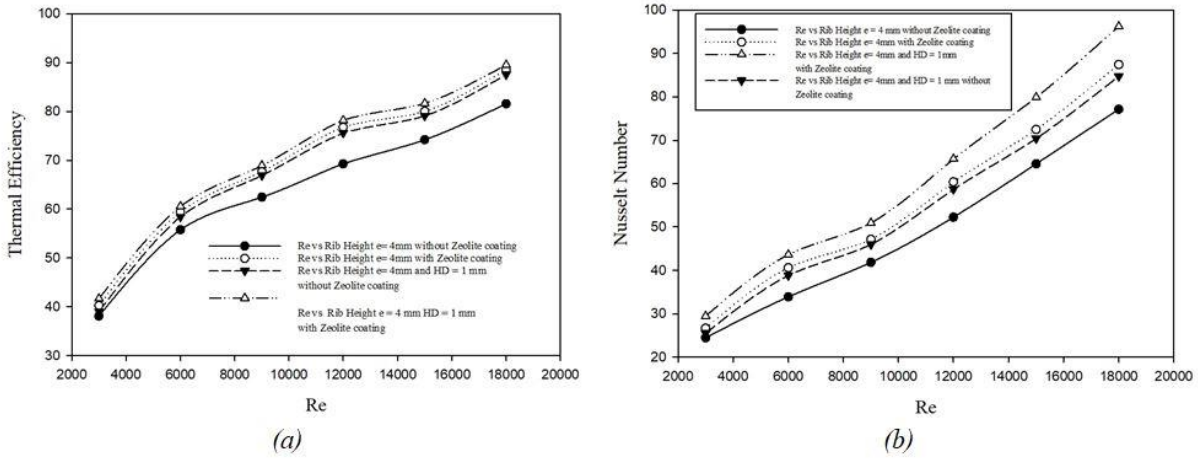
Thermal Efficiency
Re
Re vs Rib Height e= 4mm without Zeolite coating
Re vs Rib Height e= 4mm with Zeolite coating
Re vs Rib Height e= 4mm and HD = 1 mm without Zeolite coating
Re vs Rib Height e = 4 mm HD = 1 mm with Zeolite coating
(a)
Nusselt Number
Re
Re vs Rib Height e = 4 mm without Zeolite coating
Re vs Rib Height e= 4mm with Zeolite coating
Re vs Rib Height e= 4mm and HD = 1mm with Zeolite coating
Re vs Rib Height e= 4mm and HD = 1 mm without Zeolite coating
(b)

Figure 6

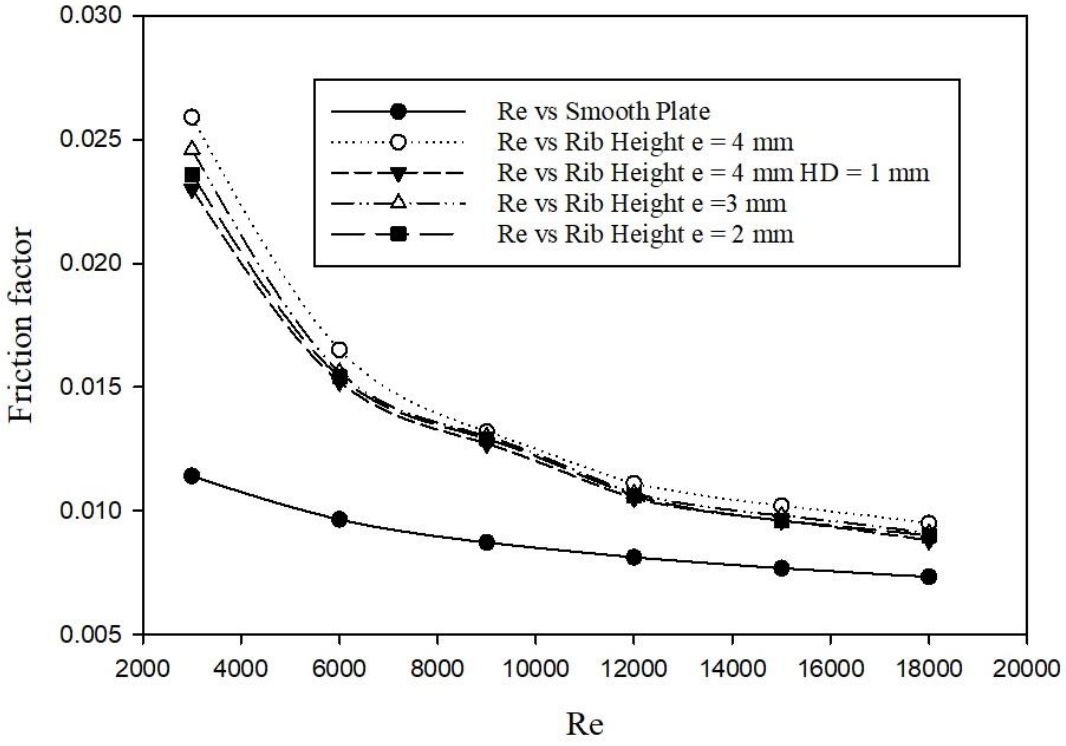
0.030
0.025
0.020
0.015
0.010
0.005
Friction factor
2000
4000
6000
8000
10000
12000
14000
16000
18000
20000
Re
Re vs Smooth Plate
Re vs Rib Height e = 4 mm
Re vs Rib Height e = 4 mm HD = 1 mm
Re vs Rib Height e =3 mm
Re vs Rib Height e = 2 mm

Figure 7